

Synthesis and Structures of Cross-Conjugated Bis-dehydroannulenes with a Y-Enediyne Motif and Different π Topologies

Arkasish Bandyopadhyay,^[a] Babu Varghese,^[b] Henning Hopf,^[c] and Sethuraman Sankararaman*^[a]

Dedicated to Professor Dr. Rolf Gleiter on the occasion of his 70th birthday

Abstract: A synthesis of cross-conjugated bis-dehydroannulenes with different topologies of the π electrons by Cu^{II} -mediated oxidative coupling of the corresponding terminal acetylenic precursors is reported. In general, of the two possible modes of cyclization, which would yield either a [13]annulene or an [18]annulene, the precursors

yielded exclusively the bis-dehydro[13]annulenes. However, one example of the formation of a bis-dehydro[18]annulene is also reported. The

Keywords: alkynes • annulenes • cross-conjugation • enediynes • macrocycles

mode of cyclization to form either the [13]annulene or the [18]annulene is explained on the basis of the conformational preference of the core unit bearing the Y-enediynes moieties. The structures of the two types of bis-annulenes have been unequivocally established by means of single-crystal X-ray crystallographic analysis.

Introduction

Extensively conjugated organic molecules are potentially useful in molecular electronics and photonics applications.^[1] The discovery of fullerenes and carbon nanotubes has created a flurry of activity in the design and synthesis of other forms of carbon allotropes, such as graphyne, graphadiyne, cyclo[n]carbons, and so on.^[2] Several model compounds bearing graphadiyne structural units have been reported.^[3] These molecules are fully conjugated dehydrobenzoannulenes that incorporate several acetylenic bridges.^[4] Dehydrobenzoannulenes of various sizes, shapes, and symmetries have been synthesized, as well as some bearing various or-

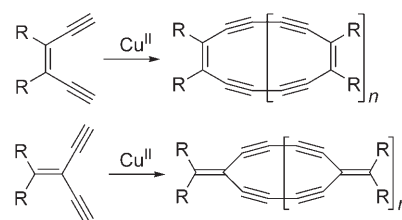
ganometallic moieties, and these exhibit interesting electronic properties.^[5] The majority of the dehydrobenzoannulenes reported to date belong to the family of linearly conjugated annulenes. The oxidative coupling of *cis*-1,2-diethynylethene and its derivatives gives dehydroannulenes with linear conjugation of the π electrons.^[6] On the other hand, oxidative coupling of 1,1-diethynylethene and its derivatives results in the formation of expanded radialenes, which may be considered as cross-conjugated dehydroannulenes^[7] (Scheme 1).

Cross-conjugated molecules exhibit unusual and interesting electronic properties^[8] that result from an alternative mode of π -electron communication, and those incorporating Y-enediynes units have been shown to exhibit interesting solvatochromic, electrochromic, and nonlinear optical (NLO) properties.^[9] Such molecules are potentially useful as organic materials in molecular electronics and photonics. Herein,

[a] A. Bandyopadhyay, Prof. Dr. S. Sankararaman
Department of Chemistry
Indian Institute of Technology Madras
Chennai 600036 (India)
Fax: (+91) 44-2257-0545
E-mail: sankar@iitm.ac.in

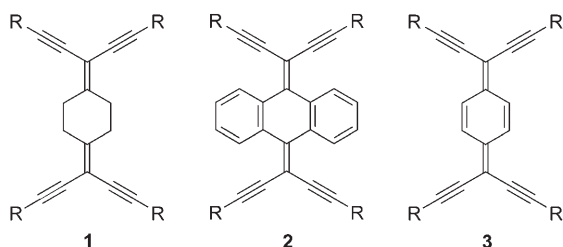
[b] Dr. B. Varghese
Sophisticated Analytical Instrument Facility
Indian Institute of Technology Madras
Chennai 600036 (India)

[c] Prof. Dr. H. Hopf
Institute of Organic Chemistry
University of Braunschweig
38106 Braunschweig (Germany)



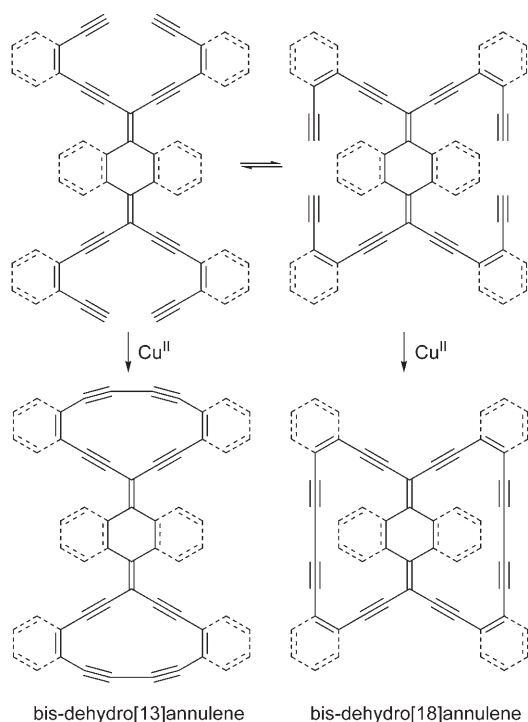
Scheme 1. Oxidative coupling of *cis*-enediynes and Y-enediynes to give linear and cross-conjugated dehydroannulenes, respectively.

we describe the synthesis of several cross-conjugated bis-dehydroannulenes. We have chosen two known bis-Y-enediynes as core units, namely 1,4-bis(1-ethynyl-2-propynylidene)cyclohexane (**1b**)^[10] and 9,10-bis(1-ethynyl-2-propynylidene)-9,10-dihydroanthracene (**2b**)^[11] (Scheme 2).



Scheme 2. Structures of bis-Y-enediynes core units. It should be noted that **3b** has yet to be synthesized. R = trimethylsilyl (TMS) for **1a**, **2a**, and **3a**; R = H for **1b**, **2b**, and **3b**.

The synthesis of fully cross-conjugated bis-Y-enediynes **3b** has yet to be accomplished.^[12] The general structures of the precursors derived from these core units are shown in Scheme 3, along with the two possible modes of cyclization to yield bis-dehydro[13]annulene and bis-dehydro[18]annulene, respectively.

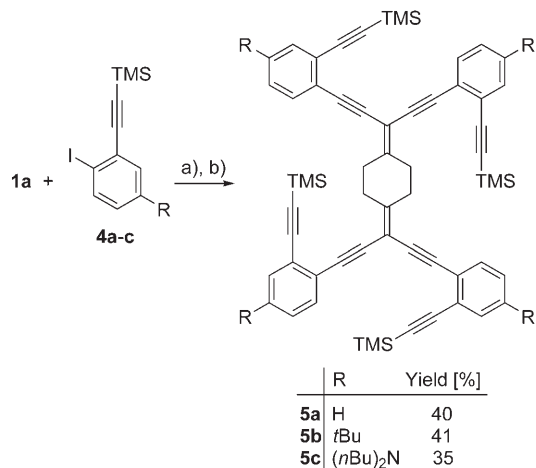


Scheme 3. Oxidative coupling of the precursor in two different modes to yield bis-dehydroannulenes of different π topologies.

Results and Discussion

Synthesis: Bis-Y-enediynyl **1b** was chosen as the precursor for the synthesis of bis-annulenes with a 1,4-cyclohexylidene

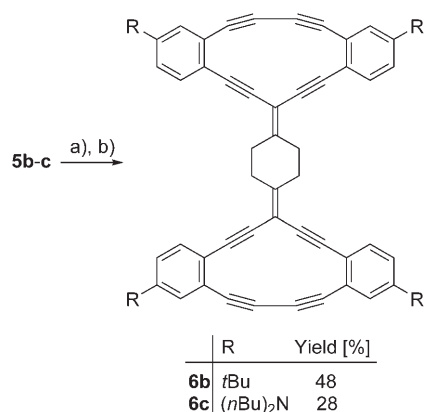
core. Tetrayne **1b** is reasonably stable and is amenable to cross-coupling reactions with iodoarenes. Sonogashira coupling of **1b**, prepared in situ from **1a**, with suitably substituted iodoarenes (**4a-c**) gave the corresponding tetrasubstituted derivatives (**5a-c**) in yields of 35–40% as yellow to red-orange solids (Scheme 4).



Scheme 4. Synthesis of precursors of bis-dehydro[13]annulenes with a 1,4-cyclohexylidene core. a) K₂CO₃, MeOH, Et₂O, RT, 3 h; b) [Pd(PPh₃)₄], CuI, *i*Pr₂NH, THF, 60 °C.

The tetrasubstituted derivatives **5a-c** were characterized by spectroscopic techniques. In the ¹H NMR spectra of **5a-c**, all eight protons of the cyclohexyl ring appeared as a sharp singlet at around δ = 2.90 to 2.96 ppm, indicating the high conformational fluxionality of this ring. This signal remained as a sharp singlet even at –60 °C. Removal of the TMS groups from **5b,c** and oxidative coupling of the resulting terminal acetylenes were accomplished in a single step to yield the corresponding bis-dehydro[13]annulenes **6b,c** in moderate yields (Scheme 5).

Bis-dehydro[13]annulenes **6b,c** were thoroughly characterized by using various spectroscopic techniques. Careful



Scheme 5. Synthesis of bis-dehydroannulenes with a cyclohexane core. a) K₂CO₃, MeOH, CH₂Cl₂, RT, 24 h; b) Cu(OAc)₂, pyridine (py), MeCN, RT, 4 days.

examination of the ^1H NMR spectra of the crude products of cyclization of **5b,c** revealed that only one type of annulene had been formed in the reaction. Only one sharp singlet was observed for all eight protons of the cyclohexyl ring in **6b,c**. Furthermore, only one set of aromatic multiplets was observed. That the oxidative cyclization of **5b,c** had yielded only [13]annulenes and not [18]annulenes (Scheme 3) was confirmed by comparing the ^1H NMR chemical shifts of the cyclohexyl protons in **5b,c** and **6b,c**. The cyclohexyl protons appeared as a sharp singlet at $\delta = 2.96$ (**5b**), 2.92 (**5c**), 2.93 (**6b**), and 2.92 ppm (**6c**), respectively. The chemical shift of the cyclohexyl protons thus remained the same before and after the cyclization. Had the cyclization proceeded to yield [18]annulenes, the cyclohexyl protons would have been relatively more shielded in **6b,c** relative to **5b,c** owing to the anisotropic effect of the ring current of the annulene ring. Only in the case of [13]annulene would the chemical shift of the cyclohexyl protons be expected to remain unaffected, in accordance with the experimental findings. Further support for the formation of [13]annulenes in the cyclization was obtained from single-crystal X-ray crystallographic analysis of **6c**,^[13] which unequivocally established the mode of cyclization (Figure 1). Oxidative cyclization of **5a** yielded a very insoluble material, which could not be purified.

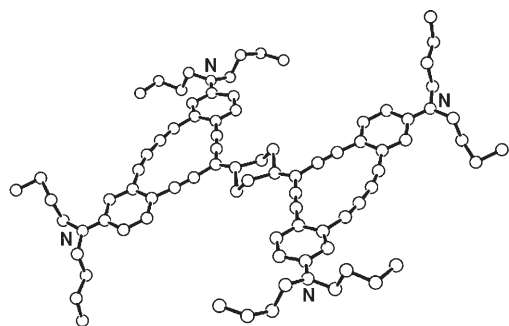
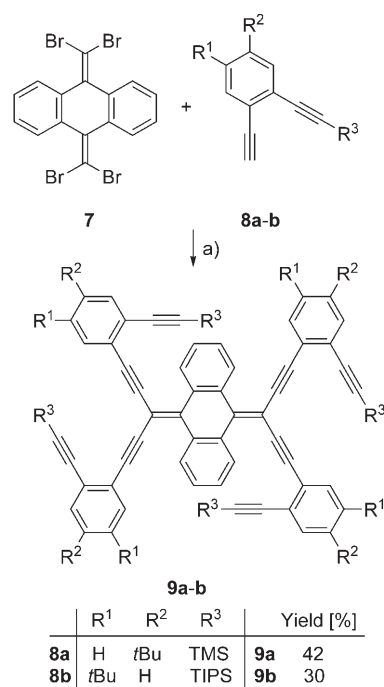


Figure 1. PLUTO representation of the structure of **6c** in the crystal, showing the chair conformation of the cyclohexylidene ring. The nitrogen atoms are labeled.

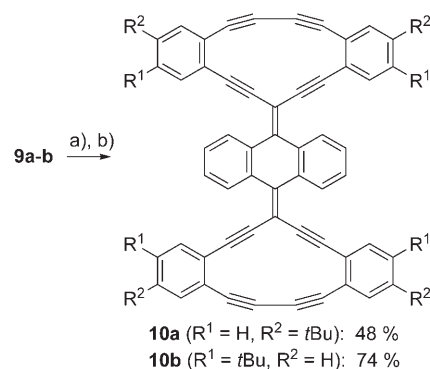
Attempted dehydrogenation of **6b,c** using 2,3-dichloro-5,6-dicyano-1,4-benzoquinone (DDQ) in refluxing toluene did not yield the desired fully cross-conjugated bis-annulenes with **3** as the core unit. Instead, only a black intractable material was obtained from these reactions.

The precursors **9a,b** for the synthesis of bis-dehydro[13]annulenes (**10a,b**) containing a 9,10-dehydroanthracene core were obtained by fourfold Sonogashira coupling of tetrabromide **7** with **8a** and **8b**, respectively (Scheme 6). Removal of the silyl protecting groups from **9a,b** followed by oxidative coupling was carried out in one pot to yield bis-dehydro[13]annulenes **10a,b** in good yields as red solids (Scheme 7).

In **9a,b** and **10a,b**, the protons on the anthracene ring appeared as a single AA'BB' pattern, indicating the symmetrical tetrasubstitution pattern in these molecules. Moreover,



Scheme 6. Synthesis of precursors of bis-dehydro[13]annulenes with a 9,10-dihydroanthracene core. a) $[\text{Pd}(\text{PPh}_3)_4]$, CuI, $i\text{Pr}_2\text{NH}$, THF, toluene, 60 °C.



Scheme 7. Synthesis of bis-dehydro[13]annulenes with a 9,10-dihydroanthracene core. a) K_2CO_3 , MeOH, CH_2Cl_2 , RT for **9a**; tetrabutyl ammonium fluoride (TBAF), MeOH, THF, RT for **9b**; b) $\text{Cu}(\text{OAc})_2$, py, MeCN, CH_2Cl_2 , RT.

as in the case of bis-[13]annulenes **6b,c**, the ^1H NMR chemical shifts of the eight anthracene ring protons remained almost the same before and after cyclization in **9a,b** and **10a,b**, respectively. For example, the anthracene ring protons appeared at $\delta = 8.60$ and 7.30 ppm in **9a** and at $\delta = 8.49$ and 7.3 ppm in **9b**, whereas the same protons appeared at $\delta = 8.47$ and 7.43 in **10a** and at $\delta = 8.55$ and 7.45 ppm in **10b** (Figure 2). It should also be noted that the introduction of bulky *tert*-butyl groups at different positions on the benzene rings in **9a** and **9b** did not alter the mode of cyclization.

Fourfold coupling of *cis*-enediynes **11** with **7** yielded precursor **12** in 24% yield (Scheme 8). The ^1H NMR spectrum of **12** displayed a single AA'BB' pattern due to the aromatic

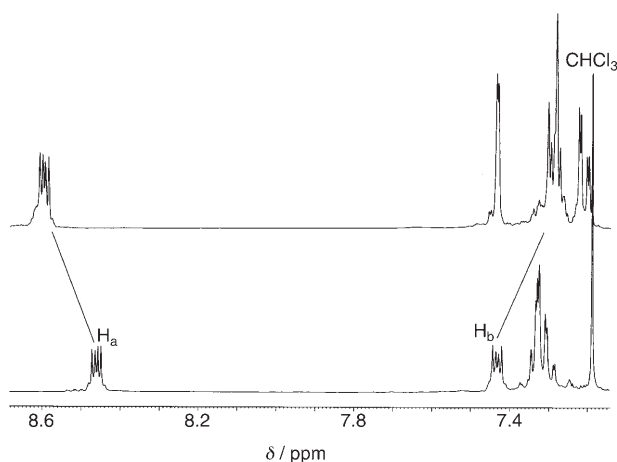
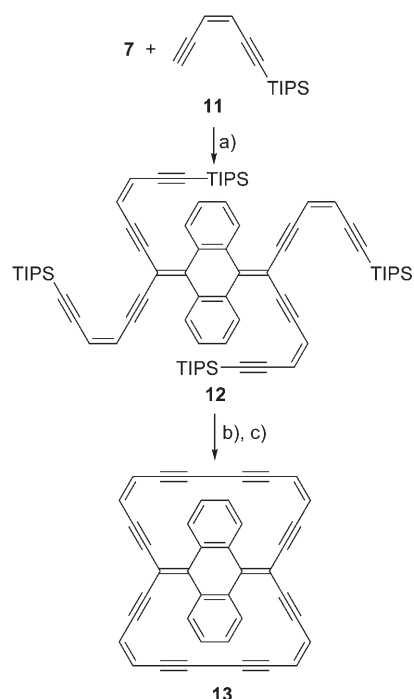


Figure 2. ^1H NMR spectra (aromatic region) of **9a** (top) and **10a** (bottom). H_a and H_b correspond to the protons on the 9,10-dihydroanthracene ring.



Scheme 8. Synthesis of bis-dehydro[18]annulene **13**. a) $[\text{Pd}(\text{PPh}_3)_4]$, CuI , $i\text{Pr}_2\text{NH}$, THF, toluene, 60°C ; b) TBAF, MeOH, THF, RT, 24 h; c) $\text{Cu}(\text{OAc})_2$, py, MeCN, CH_2Cl_2 , RT. (TIPS: triisopropylsilyl)

protons at $\delta=8.34$ and 7.28 ppm and a single AB pattern due to the olefinic protons at $\delta=5.96$ and 5.87 ppm. In situ desilylation followed by oxidative coupling using Cu^{II} yielded **13** in 40% yield (Scheme 8).

Careful examination of the ^1H NMR spectrum of the crude product clearly showed the formation of only one type of annulene, as evident from a single AA'BB' pattern due to the aromatic protons and a single AB pattern due to the olefinic protons. Furthermore, the chemical shifts of the aromatic protons showed these to be considerably more shielded in **13** than in the open precursor **12**. The aromatic

protons of **13** appeared at $\delta=7.65$ and 7.08 ppm, while those of **12** appeared at $\delta=8.34$ and 7.28 ppm, in both cases as an AA'BB' pattern (Figure 3). This clearly suggests that the

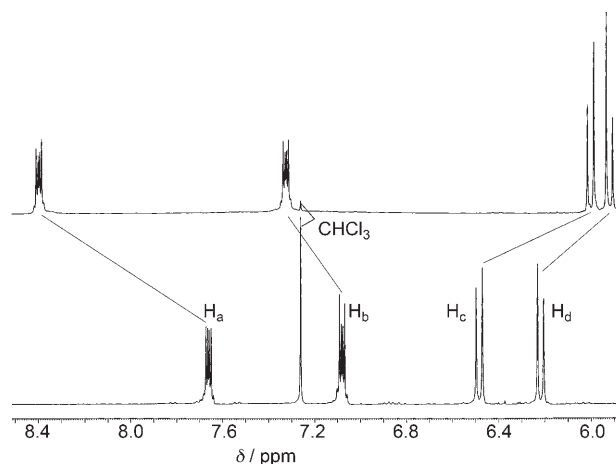


Figure 3. ^1H NMR spectra (aromatic region) of **12** (top) and **13** (bottom). H_a and H_b correspond to the protons on the 9,10-dihydroanthracene ring; H_c and H_d correspond to the olefinic protons.

cyclization had yielded a bis-dehydro[18]annulene and not a bis-dehydro[13]annulene. The shielding of the aromatic protons in **13** is due to the anisotropy effect of the ring current, which is absent in **12**. The olefinic protons of **13** appeared at $\delta=6.41$ and 6.14 ppm while those of **12** appeared at $\delta=5.89$ and 5.78 ppm, in both cases as an AB pattern (Figure 3).

Finally, bis-annulene **13** was structurally characterized by means of single-crystal X-ray diffraction analysis, which clearly showed it to be a bis-dehydro[18]annulene and not a bis-dehydro[13]annulene (Figure 4).^[13] The structure of **13** is nonplanar. The plane of the benzenoid ring lies at a distance of 4.5 \AA from the plane of the annulene ring. The structure of **13** resembles that of a recliner-chair. There are no unusual bond lengths or strained bond angles in **13**, with all pa-

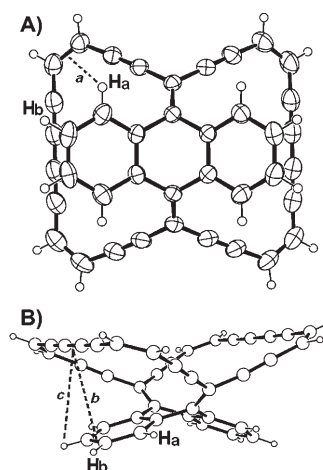


Figure 4. Structure of **13** in the crystal: A) front view in ORTEP representation; B) side view in PLUTO representation, showing the recliner-chair-like structure. Distances: $a=3.839$, $b=3.847$, $c=4.606 \text{ \AA}$.

rameters lying within the expected ranges. The distances a and c indicated in Figure 4 clearly show that the aromatic protons H_a and H_b are located at 3.8 and 4.6 Å, respectively, from the annulene π system. At these distances, which are much larger than the optimal distance for π - π interaction, the anisotropic effect of the ring current would be expected to be minimal. In fact, the distance dependence of the anisotropic effect is clearly evident, in that H_a , which lies closer to the annulene π electrons, is more shielded ($\delta=0.69$ ppm) than H_b ($\delta 0.20$ ppm). Alternatively, H_b protons that lie directly above the triple bonds could be under the influence of the deshielding effect of the anisotropy of the triple bond and the shielding effect of the ring current of the annulene π system, such that the chemical shift of H_b is the net result of these two opposing effects.

Haley and co-workers^[14] have shown that the mode of cyclization to form either bis-dehydro[14]annulenobenzene or bis-dehydro[15]annulenobenzene can be switched by changing the conditions of the oxidative cyclization. When the reactions were carried out under typical Glaser–Eglinton conditions using Cu^{II} , only the bis-[15]annulenes were formed. On the other hand, when the oxidative couplings were carried out using Pd^{II} bearing bidentate phosphane ligands, only bis-[14]annulenes were formed. The formation of these two isomeric bis-annulenes can be rationalized in terms of the geometries of the intermediate metal acetylides. In the case of Cu-mediated cyclization, a pseudo-*trans* configuration of an intermediate involving a dimeric Cu^{I} acetylide is proposed, whereas in the case of Pd-mediated cyclization, a *cis*-like geometry of the Pd^{II} acetylide is proposed. When oxidative palladium chemistry using $[\text{PdCl}_2(\text{dppe})]$ (dppe: 1,2-bis(diphenylphosphino)ethane) was employed for the cyclization of desilylated **9a,b**, under the reaction conditions reported by Haley and co-workers, we again observed the exclusive formation of **10a,b**, and none of the bis-[18]annulene. Therefore, we conclude that with these substrates the mode of cyclization is unaffected by the metal ion used. In Haley's bis-dehydroannulenes, the core ring is planar. In the present study, however, the core ring is a non-planar cyclohexane. In **1a**, the cyclohexane ring has a chair conformation,^[12] and this is also evident from the X-ray structure of **6c**. Molecular models show that in order to form the bis-dehydrobenzo[18]annulene, the cyclohexane ring must adopt either a boat or a twist-boat conformation. Furthermore, in this mode of cyclization, the conjugation is incomplete due to the methylene groups of the core ring. These factors perhaps dictate the mode of cyclization to form the bis-dehydro[13]annulene.

Tetrayne **2b** has been structurally characterized by single-crystal X-ray diffraction analysis, which clearly showed that the middle ring of the dihydroanthracene moiety has a boat-like conformation.^[15] The crystal structure of **13** also clearly revealed the boatlike geometry of the core unit. This would imply that the precursor, namely the desilylated derivative of **12**, also has a boatlike geometry of the core unit. Formation of the bis-dehydro[18]annulene **13** rather than the isomeric [13]annulene is perhaps dictated by the geometry of the core unit and the conformation of the pendant ethynyl groups in the precursor. We presume that derivatives **9a,b** also have the same geometry with respect to the dihydroanthracene ring. However, **9a,b** underwent oxidative cyclization to preferentially afford only the bis-dehydro[13]annulenes and not the corresponding bis-dehydro[18]annulenes. This would imply that the mode of cyclization of **9a** and **9b** to yield **10a** and **10b**, respectively, is dictated by the conformation of the Y-enediynes side chain rather than that of the central core anthracene ring.

Electronic absorption and emission spectroscopy: Absorption and emission spectra of the annulenes and their corresponding uncyclized precursors were recorded for sample solutions in dichloromethane (Table 1). In the cyclohexane series, the absorption maxima of the annulenes (**6b,c**) were found to be redshifted by $\lambda=50$ – 55 nm relative to those of the uncyclized precursors (**5b,c**) (Figure 5). This observation

Table 1. Absorption and emission data for bis-dehydroannulenes and their precursors.

	Absorption λ_{max} [nm] ($\log \epsilon$) in CH_2Cl_2	Emission λ_{max} [nm] in CH_2Cl_2
5a	330 (sh, 4.54), 300 (4.65), 260 (4.90), 254 (4.88), 238 (4.92)	not measured
5b	330 (sh, 4.72), 302 (4.83), 261 (5.06), 241 (5.09)	405
5c	370 (4.84), 347 (4.87), 316 (4.83), 264 (5.01), 256 (5.01)	417
6b	379 (4.49), 277 (4.95), 230 (4.83)	408, 428
6c	446 (4.58), 415 (sh, 4.47), 343 (sh, 4.87), 328 (5.13), 318 (5.13), 258 (4.61), 231 (4.88)	486
9a	423 (3.74), 359 (3.69), 237 (4.34)	447
9b	417 (3.22), 348 (3.19), 241 (3.96)	496
10a	454 (1.82), 286 (2.47)	nonfluorescent
10b	461 (3.12), 386 (3.11), 288 (3.63), 243 (3.52)	nonfluorescent
12	426 (2.83), 366 (2.79), 348 (2.96), 325 (3.00), 293 (3.18), 277 (3.21), 264 (3.20)	449
13	376 (2.66), 334 (2.76)	nonfluorescent

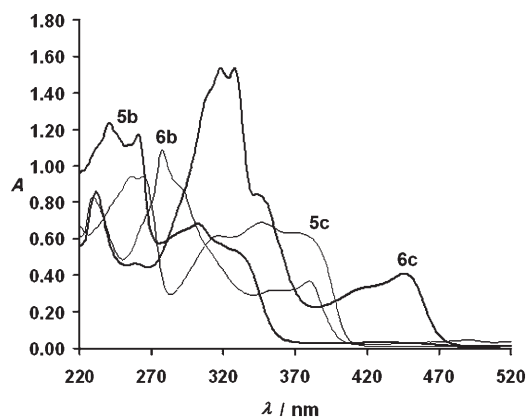


Figure 5. Comparison of the UV/Vis absorption spectra of the open precursors **5b,c** and the annulenes **6b,c** in CH_2Cl_2 (10^{-5} M).

conforms to the expected trend for annulenes in which the conjugation is complete. Among the studied annulenes, **6c**, bearing electron-donating di-*n*-butylamino substituents, shows a redshift of its absorption bands relative to those of **6b**, which bears *tert*-butyl groups. A similar trend is observed for **5b** and **5c**. Compared with the substrates with a cyclohexane core (**5b,c** and **6b,c**), those with an anthracene core (**9a,b** and **10a,b**) show a redshift of the absorption bands. In contrast to the cyclohexane series, the anthracene series has complete cross-conjugation of the two annulene rings through the anthracene unit. Therefore, the absorption bands are more redshifted in the anthracene series. Moreover, within the anthracene series, the absorption bands of the annulenes (**10a,b**) are more redshifted relative to those of the corresponding precursors (**9a,b**) (Figure 6).

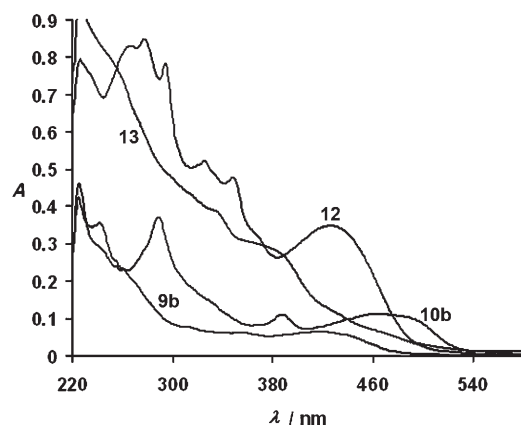


Figure 6. Comparison of the UV/Vis absorption spectra of **9b** (10^{-5} M), **10b** (10^{-4} M), **12** (5×10^{-4} M), and **13** (1.2×10^{-4} M) (in CH_2Cl_2).

Fluorescence emission spectra were measured for sample solutions in deoxygenated CH_2Cl_2 (Table 1). The fluorescence spectra of the precursors (**5b,c**) and the annulenes (**6b,c** and **9a,b**) showed a single, broad, featureless band in the region $\lambda = 350\text{--}600$ nm (Figure 7). The emission bands of

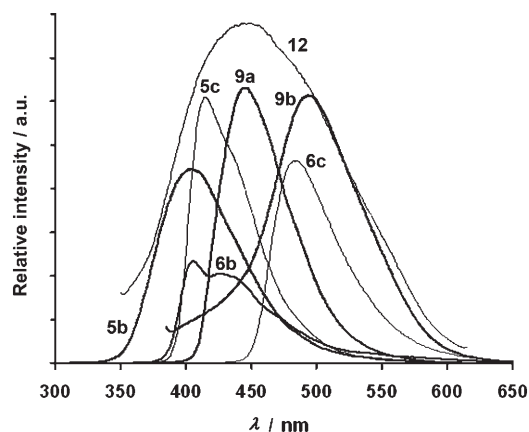


Figure 7. Fluorescence spectra in CH_2Cl_2 (10^{-4} M) of **5b** ($\lambda_{\text{ex}} = 302$ nm), **5c** ($\lambda_{\text{ex}} = 316$ nm), **6b** ($\lambda_{\text{ex}} = 350$ nm), **6c** ($\lambda_{\text{ex}} = 420$ nm), **9a** ($\lambda_{\text{ex}} = 356$ nm), **9b** ($\lambda_{\text{ex}} = 357$ nm), and **12** ($\lambda_{\text{ex}} = 322$ nm).

the substrates bearing electron-donating *N,N*-dibutylamino groups (**5c** and **6c**) showed bathochromic shifts in comparison to those of substrates bearing only *tert*-butyl groups (**5b** and **6b**). The bathochromic shift is more pronounced in the case of the annulenes than in the case of the precursors. Specifically, there is a bathochromic shift of 55 nm between **6b** ($\lambda_{\text{max}} = 431$ nm) and **6c** ($\lambda_{\text{max}} = 486$ nm), whereas the shift is only 12 nm between **5b** ($\lambda_{\text{max}} = 405$ nm) and **5c** ($\lambda_{\text{max}} = 417$ nm). Comparison of the precursors (**5b** and **5c**) and the annulenes (**6b** and **6c**) also clearly shows that the emission band of the annulenes is more redshifted than that of the precursors. Specifically, the bathochromic shift is 26 nm between **5b** and **6b** and 69 nm between **5c** and **6c**. In the case of the precursors, the phenylethynyl substituents are likely to be nonplanar. However, cyclization results in the [13]annulene ring becoming planar, thus allowing for better delocalization of the π electrons. Therefore, the annulenes show a larger bathochromic shift relative to the corresponding precursors. These observations are in line with the findings reported by Haley^[13] for linearly conjugated dehydrobenzoannulenes. The precursors **9a** ($\lambda_{\text{max}} = 447$ nm) and **9b** ($\lambda_{\text{max}} = 496$ nm) are fluorescent, and the emission of **9b** is redshifted by 49 nm in comparison with that of **9a**. In contrast, the fully cross-conjugated annulenes (**10a,b** and **13**) are not fluorescent. In fully cross-conjugated annulenes such as **10a,b** and **13**, nonradiative deactivation of the S_1 state competes effectively with fluorescence emission.^[16]

Conclusion

We have synthesized a series of cross-conjugated dehydroannulenes with either a 1,4-cyclohexane core or a 9,10-dihydroanthracene core from the corresponding terminal acetylene precursors by means of Eglinton coupling. The oxidative coupling reaction generally yielded bis-dehydro[13]annulenes as exclusive products in both series. In one case, however, it yielded a bis-dehydro[18]annulene. The [13]annulene and the [18]annulene have different π topologies. One example of each of these classes of annulenes has been structurally characterized by means of single-crystal X-ray crystallographic analysis. The electronic absorption and emission properties of this class of annulenes have been studied.

Experimental Section

General procedure for the synthesis of 5a–c: Tetrayne **1b**^[10] was prepared in situ by removal of the trimethylsilyl groups from 7,7,8,8-tetrakis(trimethylsilylethynyl)-*p*-quinodimethane (**1a**).^[17] K_2CO_3 (2.81 g, 20 mmol) was added to a degassed solution of **1a** (1.0 g, 2 mmol) in MeOH (50 mL) and diethyl ether (50 mL). The mixture was stirred under an argon atmosphere for 3 h at 25–30 °C. The solvents were then removed under reduced pressure at room temperature and the residue was added to ice-cold water (100 mL) and extracted with diethyl ether (3 × 50 mL). The combined organic extracts were washed thoroughly with saturated brine (2 × 100 mL). After drying over anhydrous Na_2SO_4 , the

solvent was removed under reduced pressure at room temperature to afford the crude tetrayne **1b**, which was redissolved in THF (20 mL). In a separate Schlenk flask, a mixture of iodoarene (12 mmol) and diisopropylamine (50 mL) was degassed by bubbling argon through it for 10 min. [Pd(PPh₃)₄] (0.23 g, 0.2 mmol) and CuI (77 mg, 0.4 mmol) were then added and the mixture was stirred at room temperature for 10 min. The solution of tetrayne **1b** in THF was then added dropwise and the mixture was heated to 60 °C and stirred for 48 h. After cooling to room temperature, the contents of the flask were diluted with CH₂Cl₂ (150 mL). The resulting solution was washed first with ice-cold 2 N HCl (3 × 100 mL) and then with saturated NH₄Cl solution (3 × 100 mL). The organic layer was dried over anhydrous Na₂SO₄ and the solvent was removed under reduced pressure. The crude product thus obtained was purified by column chromatography on silica gel, eluting with diethyl ether/hexane (5:95, v/v).

Compound 5a: Yield: 0.72 g (40%) as a yellow solid from **1a** (1.0 g, 2.0 mmol) and **4a**^[18,19,22] (3.36 g, 12.0 mmol); m.p. 180–182 °C; ¹H NMR (400 MHz, CDCl₃): δ = 7.31 (m, 8H), 7.05 (m, 8H), 2.78 (s, 8H), 0.04 ppm (s, 36H); ¹³C NMR (100 MHz, CDCl₃): δ = 158.4, 132.5, 132.0, 127.9, 127.7, 125.9, 125.3, 103.6, 100.4, 98.6, 90.5, 89.4, 32.2, -0.02 ppm; IR (neat): $\tilde{\nu}$ = 2158 cm⁻¹; UV/Vis (CH₂Cl₂): λ_{max} (log ϵ) = 330 (sh, 4.54), 300 (4.65), 260 (4.90), 254 (4.88), 238 nm (4.92); ESI-MS: *m/z* (%) = 999 (65) [M+Ag, C₆₀H₆₀Si₄Ag], 1000 (40), 1001 (100), 1002 (48), 1003 (15); HRMS: *m/z* calcd for C₆₀H₆₀Si₄Ag: 999.2823, found: 999.2795; elemental analysis calcd (%) for C₆₀H₆₀Si₄: C 80.66, H 6.77; found: C 79.23, H 6.82.

Compound 5b: Yield: 2.3 g (40.5%) as a yellow solid from **1a** (2.5 g, 5.0 mmol) and **4b**^[6c,18] (10.85 g, 30.4 mmol); m.p. 140–142 °C; ¹H NMR (400 MHz, CDCl₃): δ = 7.52 (d, 4H, *J* = 2 Hz), 7.44 (d, 4H, *J* = 8.2 Hz), 7.32 (dd, 4H, *J* = 8.2, 2 Hz), 2.96 (s, 8H), 1.34 (s, 36H), 0.25 ppm (s, 36H); ¹³C NMR (100 MHz, CDCl₃): δ = 157.9, 151.1, 131.8, 129.3, 125.4, 124.8, 123.2, 104.2, 100.5, 97.7, 90.5, 88.8, 34.7, 32.1, 31.0, 0.04 ppm; IR (neat): $\tilde{\nu}$ = 2157 cm⁻¹; UV/Vis (CH₂Cl₂): λ_{max} (log ϵ) = 330 (sh, 4.72), 302 (4.83), 261 (5.06), 241 nm (5.09); ESI-MS: *m/z* (%) = 1139 (97) [M+Na, C₇₆H₉₂Si₄Na], 1140 (100), 1141 (67), 1142 (33), 1143 (17); 1223 (63) [M+Ag, C₇₆H₉₂Si₄Ag], 1224 (65), 1225 (100), 1226 (80), 1227 (50), 1228 (25); HRMS: *m/z* calcd for C₇₆H₉₂Si₄Ag: 1223.5327, found: 1223.5328; elemental analysis calcd (%) for C₇₆H₉₂Si₄: C 81.66, H 8.30; found: C 81.71, H 8.26.

Compound 5c: Yield: 2.5 g (35%) as a reddish-orange solid from **1a** (2.5 g, 5.0 mmol) and **4c**^[18,20] (13.0 g, 30.4 mmol); m.p. 142–144 °C; ¹H NMR (400 MHz, CDCl₃): δ = 7.31 (d, 4H, *J* = 9 Hz), 6.71 (d, 4H, *J* = 2.5 Hz), 6.55 (dd, 4H, *J* = 9, 2.5 Hz), 3.29 (t, 16H, *J* = 7.3 Hz), 2.92 (s, 8H), 1.59 (q, 16H, *J* = 7.3 Hz), 1.37 (sextet, 16H, *J* = 7.3 Hz), 0.99 (t, 24H, *J* = 7.3 Hz), 0.25 ppm (s, 36H); ¹³C NMR (100 MHz, CDCl₃): δ = 147.2, 133.2, 125.9, 114.8, 112.8, 111.9, 104.9, 100.9, 96.7, 90.9, 87.4, 50.5, 32.2, 29.3, 20.2, 13.9, 0.11 ppm; IR (neat): $\tilde{\nu}$ = 2193, 2157 cm⁻¹; UV/Vis (CH₂Cl₂): λ_{max} (log ϵ) = 370 (4.84), 347 (4.87), 316 (4.83), 264 (5.01), 256 nm (5.01); ESI-MS: *m/z* (%) = 1508 (55) [M+Ag, C₉₂H₁₂₈N₄Si₄Ag], 1509 (68), 1510 (100), 1511 (87), 1512 (70), 1513 (35); HRMS: *m/z* calcd for C₉₂H₁₂₈N₄Si₄Ag: 1507.8267, found: 1507.8231.

General procedure for the synthesis of 6b,c: Solid K₂CO₃ (20 equiv) was added to a solution of the precursor (**5b** or **5c**; 1 g) in degassed MeOH (50 mL) and CH₂Cl₂ (50 mL) and the mixture was stirred for 24 h at room temperature under an argon atmosphere. A mixture of CH₃CN (75 mL) and pyridine (25 mL) was then added, followed by Cu(OAc)₂·H₂O (40 equiv). The reaction mixture was stirred at room temperature for 3 days. It was then diluted with CH₂Cl₂ (200 mL) and washed successively with 2 N HCl (3 × 200 mL) and saturated NH₄Cl solution (3 × 100 mL). The organic layer was dried over anhydrous Na₂SO₄ and the solvents were removed under reduced pressure. The crude product was purified by column chromatography on silica gel, eluting with CH₂Cl₂/hexane (1:9, v/v).

Compound 6b: Yield: 0.35 g (48%), purple solid; ¹H NMR (400 MHz, CDCl₃): δ = 7.42 (d, 4H, *J* = 8.2 Hz), 7.36 (d, 4H, *J* = 2 Hz), 7.30 (dd, 4H, *J* = 8.2, 2 Hz), 2.93 (s, 8H), 1.24 ppm (s, 36H); ¹³C NMR (100 MHz, CDCl₃): δ = 159.1, 151.6, 130.9, 127.4, 126.4, 126.2, 124.6, 100.1, 91.5, 90.7, 87.7, 80.9, 35.2, 32.9, 31.3 ppm; IR (neat): $\tilde{\nu}$ = 2195 cm⁻¹; UV/Vis (CH₂Cl₂): λ_{max} (log ϵ) = 379 (4.49), 277 (4.95), 230 nm (4.83); ESI-MS: *m/z*

(%) = 847 (100) [M+Na, C₆₄H₅₆Na], 848 (76), 849 (32); 931 (92), [M+Ag, C₆₄H₅₆Ag], 932 (62), 933 (100), 934 (61), 935 (23); HRMS: *m/z* calcd for C₆₄H₅₆Ag: 931.3433, found: 931.3407.

Compound 6c: Yield: 0.22 g (28%), dark-purple solid; m.p. 104–106 °C; ¹H NMR (400 MHz, CDCl₃): δ = 7.36 (d, 4H, *J* = 8.8 Hz), 6.61 (d, 4H, *J* = 2.7 Hz), 6.58 (dd, 4H, *J* = 8.8, 2.7 Hz), 3.26 (t, 16H, *J* = 7.2 Hz), 2.92 (s, 8H), 1.56 (q, 16H, *J* = 7.2 Hz), 1.36 (sextet, 16H, *J* = 7.2 Hz), 0.96 ppm (t, 24H, *J* = 7.2 Hz); ¹³C NMR (100 MHz, CDCl₃): δ = 154.5, 147.2, 131.9, 125.5, 116.2, 112.0, 111.3, 100.3, 91.7, 88.9, 87.7, 80.0, 50.7, 32.6, 29.3, 20.3, 13.9 ppm; IR (neat): $\tilde{\nu}$ = 2185 cm⁻¹; UV/Vis (CH₂Cl₂): λ_{max} (log ϵ) = 446 (4.58), 415 (sh, 4.47), 343 (sh, 4.87), 328 (5.13), 318 (5.13), 258 (4.61), 231 nm (4.88); ESI-MS: *m/z* (%) = 1215 (77) [M+Ag, C₈₀H₉₂N₄Ag], 1216 (68), 1217 (100), 1218 (70), 1219 (35), 1220 (12); HRMS: *m/z* calcd for C₈₀H₉₂N₄Ag: 1215.6373, found: 1215.6350.

General procedure for the synthesis of 9a,b and 12: A solution of the tetra-bromide **7** (1.0 g, 2.0 mmol) in toluene (50 mL), diisopropylamine (50 mL), and THF (30 mL) was degassed by bubbling argon through it for 10 min. [Pd(PPh₃)₄] (0.23 g, 0.2 mmol) and CuI (0.09 g, 0.46 mmol) were added and the resulting mixture was stirred for 10 min. A degassed solution of the terminal acetylene (**8a,b** or **11**; 10.0 mmol) in THF (20 mL) was then added dropwise. The reaction mixture was stirred for the specified duration at 60 °C under an argon atmosphere. After cooling to room temperature, the mixture was diluted with CH₂Cl₂ (150 mL) and washed successively with 2 N HCl (3 × 200 mL) and saturated aqueous NH₄Cl solution (3 × 100 mL). The organic layer was dried over anhydrous Na₂SO₄ and the solvents were removed under reduced pressure at room temperature. The crude product was purified by column chromatography on silica gel, eluting with CH₂Cl₂/hexane (1:19, v/v).

Compound 9a: The reaction was carried out for 48 h. The product **9a** was obtained as a dark-brown solid (1.18 g, 42%) from **7** (1.2 g, 2.3 mmol) and **8a**^[21] (2.83 g, 11.1 mmol); m.p. 152–154 °C; ¹H NMR (400 MHz, CDCl₃): δ = 8.59 (m, 4H), 7.43 (d, 4H, *J* = 1.7 Hz), 7.31 (m, 8H), 7.21 (dd, 4H, *J* = 8.2, 1.7 Hz), 1.23 (s, 36H), 0.11 ppm (s, 36H); ¹³C NMR (100 MHz, CDCl₃): δ = 151.3, 145.9, 134.3, 131.9, 129.2, 127.7, 127.3, 125.4, 125.1, 123.3, 104.1, 100.9, 98.0, 92.5, 91.8, 34.7, 31.0, 0.0 ppm; IR (neat): $\tilde{\nu}$ = 2160 cm⁻¹; UV/Vis (CH₂Cl₂): λ_{max} (log ϵ) = 423 (3.74), 359 (3.69), 237 nm (4.34); HRMS: ESI-MS *m/z* calcd for C₈₄H₉₂Si₄Ag: 1319.5327, found: 1319.5317.

Compound 9b: The reaction was carried out for 15 h. The product **9b** was obtained as a brown solid (1.2 g, 30%) from **7** (1.0 g, 1.93 mmol) and **8b** (3.93 g, 11.6 mmol); m.p. 152–155 °C; ¹H NMR (400 MHz, CDCl₃): δ = 8.49 (m, 4H), 7.35 (d, 4H, *J* = 8.1 Hz), 7.34 (s, 4H), 7.23 (m, 4H), 7.18 (dd, 4H, *J* = 8.1, 2.0 Hz), 1.19 (s, 36H), 0.96 ppm (s, 84H); ¹³C NMR (100 MHz, CDCl₃): δ = 151.0, 146.2, 134.7, 132.4, 129.1, 127.6, 127.1, 125.6, 125.4, 123.1, 105.4, 101.1, 94.4, 93.1, 91.5, 34.8, 31.1, 18.7, 11.3 ppm; IR (neat): $\tilde{\nu}$ = 2153 cm⁻¹; UV/Vis (CH₂Cl₂): λ_{max} (log ϵ) = 417 (3.22), 348 (3.19), 241 nm (3.96); ESI-MS: *m/z* (%) = 1655 (25) [M+Ag, C₁₀₈H₁₄₀Si₄Ag], 1656 (62), 1657 (100), 1658 (90), 1659 (45); HRMS: *m/z* calcd for C₁₀₈H₁₄₀Si₄Ag: 1655.9083, found: 1655.9037.

Compound 12: The reaction was carried out for 24 h. The product **12** was obtained as a red solid (0.52 g, 24%) from **7** (1.0 g, 1.94 mmol) and **11**^[22] (2.72 g, 11.6 mmol); m.p. 125–128 °C; ¹H NMR (400 MHz, CDCl₃): δ = 8.34 and 7.28 (AA'BB', 8H), 5.89 (d, 4H, *J* = 11.0 Hz), 5.78 (d, 4H, *J* = 11.0 Hz), 1.10 ppm (s, 84H); ¹³C NMR (100 MHz, CDCl₃): δ = 144.8, 133.1, 126.3, 126.2, 119.0, 118.7, 102.8, 99.5, 99.3, 94.7, 90.6, 17.6, 10.2 ppm; IR (neat): $\tilde{\nu}$ = 2140 cm⁻¹; UV/Vis (CH₂Cl₂): λ_{max} (log ϵ) = 426 (2.83), 366 (2.79), 348 (2.96), 325 (3.00), 293 (3.18), 277 (3.21), 264 nm (3.20); ESI-MS: *m/z* (%) = 1231 (50) [M+Ag, C₇₆H₁₀₀Si₄Ag], 1232 (58), 1233 (100), 1234 (70), 1235 (35); HRMS: *m/z* calcd for C₇₆H₁₀₀Si₄Ag: 1231.5953, found: 1231.5970.

Compound 10a: Precursor **9a** (0.4 g, 0.33 mmol) was dissolved in degassed MeOH (50 mL) and CH₂Cl₂ (50 mL). K₂CO₃ (0.91 g, 6.6 mmol) was added and the mixture was stirred at room temperature under an argon atmosphere for 24 h. CH₃CN (75 mL), pyridine (25 mL), and Cu(OAc)₂·H₂O (2.63 g, 1.32 mmol) were then added and the resulting mixture was stirred at room temperature for 4 days. It was then diluted with CH₂Cl₂ (200 mL) and washed successively with ice-cold 2 N HCl (3 × 200 mL) and saturated aqueous NH₄Cl solution (3 × 100 mL). The organic

layer was dried over anhydrous Na_2SO_4 and the solvents were removed under reduced pressure at room temperature. The crude product was purified by column chromatography on silica gel, eluting with CH_2Cl_2 /hexane (1:9, v/v). The product **10a** was obtained as an orange solid (0.15 g, 48 %); m.p. >240°C (decomp); ^1H NMR (400 MHz, CDCl_3): δ = 8.46 and 7.43 (AA'BB' pattern, 8H), 7.32 (m, 12H), 1.23 ppm (s, 36H); ^{13}C NMR (100 MHz, CDCl_3): δ = 150.7, 145.5, 133.8, 130.1, 127.1, 126.2, 126.1, 125.1, 124.8, 123.5, 100.1, 92.5, 91.8, 86.8, 79.9, 33.9, 29.9 ppm; IR (neat): $\tilde{\nu}$ = 2189 cm^{-1} ; UV/Vis (CH_2Cl_2): λ_{max} ($\log \epsilon$) = 454 (1.82), 286 nm (2.47); ESI-MS: m/z (%) = 1027 (80) [$M+\text{Ag}$, $\text{C}_{72}\text{H}_{56}\text{Ag}$], 1028 (62), 1029 (100), 1030 (84); HRMS: m/z calcd for $\text{C}_{72}\text{H}_{56}\text{Ag}$: 1027.3433, found: 1027.3398.

Compound 10b: Precursor **9b** (0.3 g, 0.19 mmol) was dissolved in degassed THF (30 mL), and $n\text{Bu}_4\text{NF}$ (0.3 g, 1.16 mmol) and MeOH (10 drops) were added. The mixture was stirred for 2 h at room temperature under an argon atmosphere. After removal of the solvent under reduced pressure, the concentrated reaction mixture was added to ice-cold water (100 mL) and extracted with CH_2Cl_2 (3 \times 30 mL). The combined extracts were washed thoroughly with saturated brine (2 \times 250 mL), dried over anhydrous Na_2SO_4 , and concentrated under reduced pressure to a volume of 20 mL. The concentrate was deoxygenated by bubbling argon through it. It was then added to a Schlenk flask containing a solution of $\text{Cu}(\text{OAc})_2 \cdot \text{H}_2\text{O}$ (1.54 g, 7.74 mmol) in a deoxygenated mixture of CH_3CN (75 mL) and pyridine (25 mL). After stirring at room temperature for 10 h, the mixture was diluted with CH_2Cl_2 (200 mL) and washed successively with ice-cold 2N HCl (3 \times 100 mL) and saturated NH_4Cl solution (3 \times 100 mL). The organic layer was dried over Na_2SO_4 and the solvent was removed under reduced pressure to afford the crude product. It was purified by column chromatography on silica gel, eluting with CH_2Cl_2 /hexane (1:9, v/v). **10b** was obtained as a red solid (0.13 g, 74 %); m.p. >230°C (decomp); ^1H NMR (400 MHz, CDCl_3): δ = 8.54 and 7.45 (AA'BB' pattern, 4H), 7.41 (s, 4H), 7.23 (s, 8H), 1.25 ppm (s, 36H); ^{13}C NMR (100 MHz, CDCl_3): δ = 152.0, 146.5, 134.8, 129.7, 128.5, 128.3, 127.0, 125.7, 121.9, 101.2, 93.5, 87.5, 80.9, 34.8, 30.9 ppm; IR (neat): $\tilde{\nu}$ = 2208 cm^{-1} ; UV/Vis (CH_2Cl_2): λ_{max} ($\log \epsilon$) = 461 (3.12), 386 (3.11), 288 (3.63), 243 nm (3.52); ESI-MS: m/z (%) = 1027 (56) [$M+\text{Ag}$, $\text{C}_{72}\text{H}_{56}\text{Ag}$], 1028 (73), 1029 (100), 1030 (52); HRMS: m/z calcd for $\text{C}_{72}\text{H}_{56}\text{Ag}$: 1027.3433, found: 1027.3440.

Synthesis of 13: Compound **13** was synthesized from precursor **12** (0.4 g, 0.35 mmol) according to the procedure described for the synthesis of **10b** from **9b**. **13** was obtained as a red solid (80 mg, 40 %); m.p. >210°C (decomp); ^1H NMR (400 MHz, CDCl_3): δ = 7.59 and 7.02 (AA'BB' pattern), 6.41 (d, 4H, J = 10.5 Hz), 6.14 ppm (d, 4H, J = 10.5 Hz); ^{13}C NMR (100 MHz, CDCl_3): δ = 151.1, 132.6, 129.0, 127.3, 121.5, 118.5, 99.9, 96.5, 92.9, 80.9, 80.7 ppm; IR (neat): $\tilde{\nu}$ = 2923, 2853, 1050, 794 cm^{-1} ; UV/Vis (CH_2Cl_2): λ_{max} ($\log \epsilon$) = 376 (2.66), 334 (2.76), 242 nm (3.03); ESI-MS: m/z (%) = 603 (80) [$M+\text{Ag}$, $\text{C}_{40}\text{H}_{16}\text{Ag}$], 604 (26), 605 (82), 606 (30); HRMS: m/z calcd for $\text{C}_{40}\text{H}_{16}\text{Ag}$: 603.0303, found: 603.0306.

Compound 8b: A solution of **8a**^[21] (6.0 g, 17.0 mmol) in diisopropylamine (50 mL) and THF (50 mL) was degassed by bubbling argon through it for 10 min. $[\text{Pd}(\text{PPh}_3)_4]$ (0.2 g, 0.17 mmol) and CuI (0.064 g, 0.34 mmol) were added, and the resulting mixture was stirred for 10 min at room temperature. Triisopropylsilylacetylene (4.17 mL, 18.5 mmol) was then added and the mixture was stirred at room temperature for 12 h. The reaction mixture was then diluted with CH_2Cl_2 (100 mL) and washed successively with ice-cold 2N HCl (3 \times 100 mL) and saturated NH_4Cl solution (3 \times 100 mL). The organic layer was dried over Na_2SO_4 and the solvents were removed under reduced pressure at room temperature. The crude product was purified by column chromatography on silica gel using hexane as the eluent to yield 4-*tert*-butyl-1-triisopropylsilyl-2-trimethylsilyl-1-ethynylbenzene (6.51 g, 94 %) as a red liquid. ^1H NMR (400 MHz, CDCl_3): δ = 7.36 (d, 1H, J = 1.8 Hz), 7.27 (d, 1H, J = 8.2 Hz), 7.13 (dd, 1H, J = 8.2, 1.8 Hz), 1.16 (s, 9H), 1.05 (s, 18H), 0.98 (s, 3H), 0.15 ppm (s, 9H); ^{13}C NMR (100 MHz, CDCl_3): δ = 151.2, 132.7, 129.7, 125.3, 125.1, 123.1, 105.5, 104.1, 97.2, 93.8, 34.6, 30.9, 18.8, 11.4, 0.00 ppm; IR (neat): $\tilde{\nu}$ = 2155, 2062 cm^{-1} ; ESI-MS: m/z calcd for $\text{C}_{26}\text{H}_{42}\text{Si}_2\text{Na}$: 433.2723, found: 433.2733.

K_2CO_3 (4.04 g, 29.2 mmol) was added to a stirred solution of 4-*tert*-butyl-1-triisopropylsilyl-2-trimethylsilyl-1-ethynylbenzene (6.0 g, 14.6 mmol) in degassed MeOH (50 mL) and diethyl ether (50 mL) under an argon atmosphere at room temperature. The mixture was stirred for 1 h and then the solvents were removed under reduced pressure at room temperature. The crude product was poured into ice-cold water (100 mL) and extracted with CH_2Cl_2 (3 \times 50 mL). The combined organic layers were dried with Na_2SO_4 and the solvent was removed under reduced pressure at room temperature. The crude product was purified by column chromatography on silica gel using hexane as the eluent to yield **8b** (4.55 g, 92 %) as a red liquid. ^1H NMR (400 MHz, CDCl_3): δ = 7.50 (d, 1H, J = 2.0 Hz), 7.40 (dd, 1H, J = 8.2, 2.0 Hz), 7.30 (d, 1H, J = 8.2 Hz), 3.22 (s, 1H), 1.30 (s, 9H), 1.13 ppm (s, 21H); ^{13}C NMR (100 MHz, CDCl_3): δ = 151.2, 132.7, 129.7, 125.3, 125.1, 123.1, 105.5, 104.1, 97.2, 93.8, 34.6, 30.9, 18.8, 11.4, 0.00 ppm; IR (neat): $\tilde{\nu}$ = 2155 cm^{-1} ; ESI-MS: m/z calcd for $\text{C}_{23}\text{H}_{35}\text{Si}$: 339.2508, found: 339.2515.

Acknowledgements

We thank the DAAD, New Delhi, for financial support for A.B. to carry out part of the research at the Institute of Organic Chemistry, TU-Braunschweig, Germany. Financial support from the CSIR, New Delhi, is gratefully acknowledged. We thank the SAIF, IIT Madras, for spectral data and Mr. G. Venkataramana for a sample of **8a**.

- [1] a) J. M. Tour, *Acc. Chem. Res.* **2000**, *33*, 791–804; b) D. K. James, J. M. Tour, *Chem. Mater.* **2004**, *16*, 4423–4435; c) F. Diederich, *Nature* **1994**, *369*, 199–207; d) J. M. Tour, *Chem. Rev.* **1996**, *96*, 537–562.
- [2] a) *Acetylene Chemistry: Chemistry, Biology and Material Science* (Eds.: F. Diederich, P. J. Stang, R. R. Tykwinski), Wiley-VCH, Weinheim, **2004**; b) U. H. F. Bunz, Y. Rubin, Y. Tobe, *Chem. Soc. Rev.* **1999**, *28*, 107–119; c) F. Diederich, Y. Rubin, *Angew. Chem.* **1992**, *104*, 1123–1146; *Angew. Chem. Int. Ed. Engl.* **1992**, *31*, 1101–1123; d) H. L. Anderson, R. Faust, Y. Rubin, F. Diederich, *Angew. Chem.* **1994**, *106*, 1427–1429; *Angew. Chem. Int. Ed. Engl.* **1994**, *33*, 1366–1368; e) M. B. Nielson, F. Diederich, *Chem. Rev.* **2005**, *105*, 1837–1867.
- [3] a) Y. Rubin, F. Diederich, in *Stimulating Concepts in Chemistry* (Eds.: F. Vögtle, J. F. Stoddart, M. Shibasaki), Wiley-VCH, Weinheim, **2000**, pp. 163–186; b) F. Diederich, *Chem. Commun.* **2001**, 219–227; c) C. S. Jones, M. J. O'Connor, M. M. Haley, in *Acetylene Chemistry: Chemistry, Biology and Material Science* (Eds.: F. Diederich, P. J. Stang, R. R. Tykwinski), Wiley-VCH, Weinheim, **2004**, pp. 303–385.
- [4] a) I. Hisaki, M. Sonoda, Y. Tobe, *Eur. J. Org. Chem.* **2006**, 833–847; b) Y. Tobe, M. Sonoda, in *Modern Cyclophane Chemistry* (Eds.: R. Gleiter, H. Hopf), Wiley-VCH, Weinheim, **2004**, pp. 1–40.
- [5] For reviews, see: a) J. A. Marsden, G. J. Palmer, M. M. Haley, *Eur. J. Org. Chem.* **2003**, 2355–2369; b) M. M. Haley, J. J. Park, S. C. Brand, *Top. Curr. Chem.* **1999**, *201*, 81–130; see also: c) H. Hinrichs, A. K. Fischer, P. G. Jones, H. Hopf, M. M. Haley, *Org. Lett.* **2005**, *7*, 3793–3795; d) J. A. Marsden, M. J. O'Connor, M. M. Haley, *Org. Lett.* **2004**, *6*, 2385–2388; e) D. B. Kimball, M. M. Haley, R. H. Mitchell, T. R. Ward, S. Bandyopadhyay, R. V. Williams, J. R. Armantrout, *J. Org. Chem.* **2002**, *67*, 8798–8811; for reviews, see: f) U. H. F. Bunz, *Chem. Rev.* **2000**, *100*, 1605–1644; g) U. H. F. Bunz, *Top. Curr. Chem.* **1999**, *201*, 131–161; see also: h) M. Laskoski, G. Roidl, M. D. Smith, U. H. F. Bunz, *Angew. Chem.* **2001**, *113*, 1508–1511; *Angew. Chem. Int. Ed. Engl.* **2001**, *40*, 1460–1463; i) M. Laskoski, M. D. Smith, J. G. M. Morton, U. H. F. Bunz, *J. Org. Chem.* **2001**, *66*, 5174–5181.
- [6] a) J. A. Antony, C. B. Knobler, F. Diederich, *Angew. Chem.* **1993**, *105*, 437–440; *Angew. Chem. Int. Ed. Engl.* **1993**, *32*, 406–409; b) W. H. Okamura, F. Sondheimer, *J. Am. Chem. Soc.* **1967**, *89*,

- 5991; c) W. B. Wan, M. M. Haley, *J. Org. Chem.* **2001**, *66*, 3893–3901; d) M. E. Gallagher, J. A. Antony, *Tetrahedron Lett.* **2001**, *42*, 7533–7536; e) S. Ott, R. Faust, *Synlett* **2004**, 1509–1512; f) Q. Zhou, T. M. Swager, *Polym. Prepr. Am. Chem. Soc. Div. Polym. Chem.* **1993**, *34*, 193–194.
- [7] a) M. B. Nielson, M. Schreiber, Y. G. Baek, P. Seiler, S. Lecomte, C. Boudon, R. R. Tykwinski, J.-P. Giesselbrecht, V. Gramlich, P. J. Skinner, C. Bosshard, P. Günther, M. Gross, F. Diederich, *Chem. Eur. J.* **2001**, *7*, 3263–3280; b) Y. Tobe, R. Umeda, N. Iwasa, M. Sonoda, *Chem. Eur. J.* **2003**, *9*, 5549–5559; c) S. Eisler, R. R. Tykwinski, *Angew. Chem.* **1999**, *111*, 2138–2141; *Angew. Chem. Int. Ed.* **1999**, *38*, 1940–1943; d) A. M. Boldi, F. Diederich, *Angew. Chem.* **1994**, *106*, 482–485; *Angew. Chem. Int. Ed. Engl.* **1994**, *33*, 468–471.
- [8] H. Hopf, *Classics in Hydrocarbon Chemistry*, Wiley-VCH, Weinheim, **2000**, Chapter 11, pp. 251–320.
- [9] a) G. T. Hwang, H. S. Son, J. K. Ku, B. H. Kim, *J. Am. Chem. Soc.* **2003**, *125*, 11242–11248; b) B. R. Kaafarani, B. Wex, F. Wang, O. Catanescu, L. C. Chien, D. C. Neckers, *J. Org. Chem.* **2003**, *68*, 5377–5380; c) S. Ito, H. Inabe, N. Morita, A. Tajiri, *Eur. J. Org. Chem.* **2004**, 1774–1780.
- [10] H. Hopf, J. Kampen, P. Bubenitschek, P. G. Jones, *Eur. J. Org. Chem.* **2002**, 1708–1721.
- [11] P. M. Donovan, L. T. Scott, *J. Am. Chem. Soc.* **2004**, *126*, 3108–3112.
- [12] Attempted conversion of **1a** to **3a** using DDQ failed. Dehydrogenation proceeded only partially to yield the corresponding dihydro derivative. See ref. [10].
- [13] X-ray crystallographic data for **6c**: Data were collected on an Enraf-Nonius CAD4 diffractometer by using Mo_Kα radiation ($\lambda = 0.71073 \text{ \AA}$) at 293 K. Crystal data: monoclinic; space group *C2/c*; $a = 25.5231(19)$, $b = 9.2830(5)$, $c = 31.004(2) \text{ \AA}$; $V = 7155.4(8) \text{ \AA}^3$; $\alpha = \gamma = 90^\circ$, $\beta = 103.074(4)^\circ$; $Z = 4$. Data collection: a crystal of approximate dimensions $0.3 \times 0.2 \times 0.2 \text{ mm}$ was used to record 6305 intensities, $2\theta_{\text{max}} = 25^\circ$, completeness to $\theta = 25^\circ$ was 100%. Structure refinement: the structure was refined anisotropically by full-matrix least-squares on F^2 to $wR2 = 0.3342$, $R1 = 0.1336$ for 400 parameters and 24 restraints. X-ray crystallographic data for **13**: Data were collected on an Enraf-Nonius CAD4 diffractometer by using Mo_Kα radiation ($\lambda = 0.71073 \text{ \AA}$) at 293 K. Crystal data: monoclinic; space group *C2/c*; $a = 23.5607(6)$, $b = 8.2705(2)$, $c = 28.4402(8) \text{ \AA}$; $V = 5384.3(2) \text{ \AA}^3$; $\alpha = \gamma = 90^\circ$, $\beta = 103.695(3)^\circ$; $Z = 8$. Data collection: a crystal of approximate dimensions $0.3 \times 0.2 \times 0.2 \text{ mm}$ was used to record 6984 intensities, $2\theta_{\text{max}} = 28.77^\circ$, completeness to $\theta = 28.77^\circ$ was 99.9%. Structure refinement: the structure was refined anisotropically by full-matrix least-squares on F^2 to $wR2 = 0.1095$, $R1 = 0.0434$ for 362 parameters and zero restraints. CCDC-622536 (**6c**) and CCDC-621595 (**13**) contain the supplementary crystallographic data for this paper. These data can be obtained free of charge from the Cambridge Crystallographic Data Centre via www.ccdc.cam.ac.uk/data_request/cif.
- [14] a) J. A. Marsden, J. J. Miller, M. M. Haley, *Angew. Chem.* **2004**, *116*, 1726–1729; *Angew. Chem. Int. Ed.* **2004**, *43*, 1694–1697; b) J. A. Marsden, J. J. Miller, L. D. Shirtcliff, M. M. Haley, *J. Am. Chem. Soc.* **2005**, *127*, 2464–2476.
- [15] See the Supporting Information of ref. [11] for the crystal structure data of **2a**.
- [16] N. J. Turro, *Modern Molecular Photochemistry*, The Benjamin/Cummings Publishing Co., Menlo Park, **1978**, Chapters 5 and 6.
- [17] a) R. Neidlein, M. Winter, *Synthesis* **1998**, 1362–1366; b) see also ref. [10].
- [18] a) H. Hinrichs, A. J. Boydston, P. G. Jones, K. Hess, R. Herges, M. M. Haley, H. Hopf, *Chem. Eur. J.* **2006**, *12*, 7103–7115; b) H. Hinrichs, Ph.D. Dissertation, TU-Braunschweig, **2005**.
- [19] J. M. Kehoe, J. H. Kiley, J. J. English, C. A. Johnson, R. C. Petersen, M. M. Haley, *Org. Lett.* **2000**, *2*, 969–972.
- [20] J. J. Pak, T. J. R. Weakley, M. M. Haley, *J. Am. Chem. Soc.* **1999**, *121*, 8182–8192.
- [21] M. Laskoski, G. Roidl, H. L. Ricks, J. S. M. Morton, M. D. Smith, U. H. F. Bunz, *J. Organomet. Chem.* **2003**, *673*, 13–24.
- [22] Y. F. Lu, C. W. Harwing, A. G. Fallis, *J. Org. Chem.* **1993**, *58*, 4202–4204.

Received: October 24, 2006
Published online: January 16, 2007